Rock Mechanics Bulletin 2 (2023) 100081

Contents lists available at ScienceDirect

Rock Mechanics Bulletin

journal homepage: www.keaipublishing.com/en/journals/rock-mechanics-bulletin

Prediction of uniaxial compressive strength of rock based on lithology using stacking models

Zida Liu [a], Diyuan Li [a,*], Yongping Liu [b], Bo Yang [a], Zong-Xian Zhang [c]

[a] School of Resources and Safety Engineering, Central South University, Changsha, 410083, China
[b] Nickel Cobalt Research and Design Institute, Jinchuan Group Co., Ltd., Jinchang, 737104, China
[c] Oulu Mining School, University of Oulu, Oulu, Finland

ARTICLE INFO

Keywords:
Uniaxial compressive strength
Point load strength
P-wave velocity
Schmidt hammer rebound number
Stacking models

ABSTRACT

Uniaxial compressive strength (UCS) of rock is an essential parameter in geotechnical engineering. Point load strength (PLS), P-wave velocity, and Schmidt hammer rebound number (SH) are more easily obtained than UCS and are extensively applied for the indirect estimation of UCS. This study collected 1080 datasets consisting of SH, P-wave velocity, PLS, and UCS. All datasets were integrated into three categories (sedimentary, igneous, and metamorphic rocks) according to lithology. Stacking models combined with tree-based models and linear regression were developed based on the datasets of three rock types. Model evaluation showed that the stacking model combined with random forest and linear regression was the optimal model for three rock types. UCS of metamorphic rocks was less predictable than that of sedimentary and igneous rocks. Nonetheless, the proposed stacking models can improve the predictive performance for UCS of metamorphic rocks. The developed predictive models can be applied to quickly predict UCS at engineering sites, which benefits the rapid and intelligent classification of rock masses. Moreover, the importance of SH, P-wave velocity, and PLS were analyzed for the estimation of UCS. SH was a reliable indicator for UCS evaluation across various rock types. P-wave velocity was a valid parameter for evaluating the UCS of igneous rocks, but it was not reliable for assessing the UCS of metamorphic rocks.

1. Introduction

Uniaxial compressive strength (UCS) is a crucial rock index extensively applied in mining, underground tunnels, reservoirs, and other rock engineering projects. Blasting, excavation, support, etc. need UCS to guide project construction and ensure production safety in the field. Additionally, many rock mass classification systems are built on the UCS, including rock mass rating (RMR) (Bieniawski, 1974), rock mass index (RMi) (Palmström, 1996), Hoek–Brown failure criterion (Hoek et al., 2002). These investigations suggest that UCS is an indispensable rock parameter in geotechnical engineering.

The rock mechanics test is a direct approach to measure the UCS (Hatheway, 2009). Rock blocks are made into standard specimens, which are loaded on the test machine until they break. The failure load and cross-section of the specimen are recorded, and the UCS is obtained by calculation. Nevertheless, this process consumes considerable time to prepare the rock specimens. In particular, with the mining of deep mineral resources, it is challenging to acquire intact rock samples from highly stressed and fractured rock masses in deep strata (Xiao et al., 2021). Fig. 1 shows the drilling cores at different depths in a deep mine in China. Core disking makes it almost impossible to obtain intact rock blocks. In this case, it is very difficult to measure the UCS directly. Accordingly, it is significant to develop indirect evaluation methods for obtaining the UCS of rock in engineering sites (Aladejare et al., 2021).

Physical and easily obtained mechanical parameters have been considered to evaluate UCS indirectly. Physical parameters include the Equotip hardness number (L) (Corkum et al., 2018), Schmidt Hammer rebound number (SH) (Heidari et al., 2018), Shore hardness (Dinçer et al., 2008), density (ρ) (Aliyu et al., 2019), porosity (n) (Fereidooni, 2016), P-wave velocity (V_P) (Rahman and Sarkar, 2021), S-wave velocity (V_S) (Uyanık et al., 2019), unit weight (γ) (Török and Vásárhelyi, 2010), slake durability index (SDI) (Sharma et al., 2017), etc. Mechanical parameters utilized to estimate the UCS are more readily measurable than the UCS. These parameters comprise the block punch index (BPI) (Heidari et al., 2018), Young's modulus (E) (Najibi et al., 2015), Poisson ratio (ν), Brazilian tensile strength (BTS) (Aliyu et al., 2019), point load

* Corresponding author.
E-mail address: diyuan.li@csu.edu.cn (D. Li).

https://doi.org/10.1016/j.rockmb.2023.100081
Received 5 August 2023; Received in revised form 2 September 2023; Accepted 9 September 2023
Available online 11 September 2023

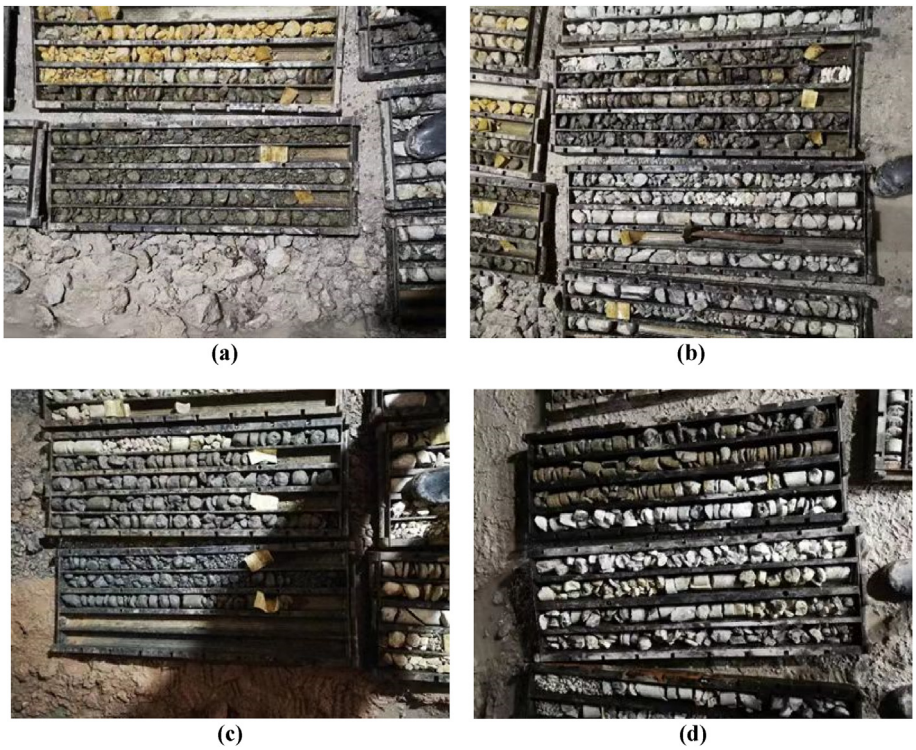

Fig. 1. Drilling cores at different depths in a deep mine in China: (a) 1050 m; (b) 1150 m; (c) 1200 m; (d) 1250 m.

strength (PLS) (Aliyu et al., 2019; Fereidooni, 2016), and other properties.

Among the physical and mechanical parameters, PLS, V_P, and SH are easily measured on-site (Armaghani et al., 2016a). They have a close relationship with rock properties. For instance, PLS has been recommended as an indirect measure of UCS owing to its testing ease, simplicity of specimen preparation, and field applications (Kahraman, 2001). V_P represents the propagation velocity of elastic waves in rocks, which is closely associated with rock properties (Wei et al., 2022). SH is implemented to test the quality of rock, which can be measured by the Schmidt hammer (Wang and Wan, 2019). PLS, V_P, and SH frequently serve to indirectly evaluate UCS owing to their practicality and simplicity.

Numerous intelligent algorithms have been extensively applied to predict UCS based on physical and easily obtained mechanical parameters. Table 1 lists intelligent techniques for predicting UCS of rock in recent years. Neural network models (ANN, ANFIS, RBFN, and ELM) are popular for UCS prediction owing to their ability to simulate complex relationships (Barham et al., 2020; Cao et al., 2022; Miah et al., 2020; Teymen and Mengüç, 2020), but training and optimizing them are computationally intensive. Hybrid models (such as ANN-GA) employ optimization algorithms to enhance model performance by optimizing parameters (Ebdali et al., 2020). Ensemble models combine predictions from multiple models to improve performance by reducing errors and generating a more accurate final output (Barzegar et al., 2020). Support vector machines effectively handle high-dimensional data and produce reliable results, even with small training datasets (Shahri et al., 2022). Tree-based models (RF and XGB) are also quite useful in UCS prediction (Abdelhedi et al., 2023; Wang et al., 2023), and they are easy to use and can get good performance without hyperparameter tuning. Deep learning methods (CNN and LSTM) extract features and capture complex patterns automatically, and they are suitable for complex datasets (Mahmoodzadeh et al., 2021; Sun et al., 2021). Additionally, some other models (GEP and GPR) are also applied for the estimation of UCS (Mahmoodzadeh et al., 2021; Zhao et al., 2022).

Intelligent techniques have demonstrated a marked advantage in predicting the UCS of rock due to their ability to capture complex relationships between variables. Nevertheless, intelligent techniques are based on data-driven methods, and their capabilities mainly rely on the characteristics of the datasets (such as size, complexity, and quality). Many existing studies used limited datasets to develop predictive models of UCS. The size and quality of the datasets dictate that the developed predictive models are only suitable for specific cases and are not universally applicable. Moreover, lithology also has an impact on the assessment of UCS (Aladejare et al., 2021; Rahman and Sarkar, 2021). Incorporating lithology and multiple parameters (such as PLS, V_P, and SH) can improve the performances and applicabilities of predictive models. However, most current studies do not consider the effect of lithology on the prediction of UCS. Not only that, the datasets related to rock parameters, used in developing the predictive model of UCS, frequently exhibit both linear and non-linear patterns (Mahmoodzadeh et al., 2021, 2022; Moussas and Diamantis, 2021; Parsajoo et al., 2021). The inherent complexity of the datasets requires powerful modeling techniques. To address these limitations, this study considered the effect of lithology on rock strength and used multiple variables (PLS, V_P, and SH) to predict UCS. Meanwhile, a comprehensive database with 1080 datasets composed of PLS, V_P, SH, and UCS were collected. Large data size can provide comprehensive information about rock characteristics and reduce the randomness of the predictions. Additionally, novel stacking models suitable for rock parameter datasets that present both linear and non-linear trends were proposed to process PLS, V_P, and SH to predict UCS of different lithologies.

These collected datasets were integrated into three databases (sedimentary, igneous, and metamorphic rocks) according to lithology. For each database, the optimal distributions of PLS, V_P, SH, and UCS were determined through the Kolmogorov-Smirnov (K–S) test. Simple regression analysis was conducted to analyze the relationship between PLS, V_P, SH, and UCS. Moreover, stacking models combining tree-based models and linear regression were developed based on the collected datasets of three rock types. These stacking models were then evaluated and compared. Finally, the importance of PLS, V_P, and SH was analyzed for predicting UCS in three rock types.

Table 1
Intelligent algorithms for the prediction of UCS in recent years.

No.	Model	Input variables
1	ANN (Barham et al., 2020)	V_P, SH, BTS, ρ_{dry}, SDI, and PLS
2	Ensemble models (Barzegar et al., 2020)	V_P, SH, n, and PLS
3	ANN-GA, ANN-ICA, ANN-PSO (Ebdali et al., 2020)	ρ, V_P, Vs, and BTS
4	ANN and SVM (Miah et al., 2020)	Resistivity, gamma ray, bulk density, n, and sonic time
5	SVM-FMA (Shahri et al., 2022)	ρ, n, V_P, water absorption, and PLS
6	ANN, ANFIS, and GEP (Teymen and Mengüç, 2020)	γ, BTS, SH, L, PLS, and V_P
7	RF (Wang et al., 2020)	SH and V_P
8	ANN, ANFIS, and SVM (Gowida et al., 2021)	Rate of penetration, mud pumping rate, standpipe pressure, rotary speed in revolution per minute, torque, and weight on bit.
9	ANFIS-SFS (Jing et al., 2021)	V_P, PLS, and SH
10	LSTM, DNN, KNN, GPR, SVM, DT (Mahmoodzadeh et al., 2021)	n, SH, V_P, and PLS
11	ANN and ALPS-GP (Özdemir, 2022)	n, SH, and V_P
12	CNN (Sun et al., 2021)	CT image data
13	XGB-FA, SVM, and RBFN (Cao et al., 2022)	ρ_{dry}, V_P, quartz, plagioclase, chlorite, alkali feldspar, and mica
14	GPR (Zhao et al., 2022)	SH, V_P, PLS, n
15	PSO-RF (Wang et al., 2023)	SH, V_P, PLS, ρ
16	TSO-RF (Li et al., 2022b)	SH, V_P, PLS, ρ, n
17	ANN (Li et al., 2022b)	ρ
18	DFNN (Zhao et al., 2023)	Drilling jumbo measurement data
19	GWO-ELM (Jin et al., 2022)	SH, V_P, PLS, n
20	XGB (Abdelhedi et al., 2023)	V_P, ρ, n

Note: ANN = artificial neural network; GA = genetic algorithm; ICA = imperialist competitive algorithm; PSO = particle swarm optimization; SVM = support vector machine; FMA = firefly metaheuristic algorithm; ANFIS = adaptive neuro fuzzy inference system; GEP = gene expression programming; RF = random forest; SFS = stochastic fractal search algorithm; LSTM = long short term memory; DNN = deep neural networks; KNN = k-nearest neighbors; GPR = Gaussian process regression; DT = decision tree; ALSP = artificial intelligence-based age-layered population structure; GP = genetic programming; CNN = convolutional neural network; XGB = extreme gradient boosting; FA = firefly algorithm; RBFN = radial basis function neural network; TSO = transient search optimization; DFNN = deep feedforward neural network; ELM = extreme learning machines; GWO = grey wolf optimization.

2. Data

2.1. Data collection of rock samples

This study collected 1080 rock samples from 18 studies published between 1999 and 2022 (Armaghani et al., 2016b; Çobanoğlu and Çelik, 2008; Dehghan et al., 2010; Diamantis and Moussas, 2021; Dinçer et al., 2008; Güneyli et al., 2022; Heidari et al., 2018; Kahraman, 2001; Kallu and Roghanchi, 2015; Kılıç and Teymen, 2008; Kurtuluş et al., 2016; Mahmoodzadeh et al., 2021; Mishra and Basu, 2013; Momeni et al., 2015; Ng et al., 2015; Tandon and Gupta, 2015; Teymen and Mengüç, 2020; Tuğrul and Zarif, 1999). PLS, V_P, SH, and UCS were measured for each sample. The detailed data and rock type can be found in the supplemental data. In the collected datasets, SH was measured by L and N-type Schmidt hammers, in which the impact energy was different. Asteris et al. (2021) applied the least square methods to fit the relationship between L and N-type SH in rocks. Eq. (1) displays the result, which receives a correlation coefficient (R) of 0.96. This study employs Eq. (1) to convert N-type SH to L-type SH. Fig. 2 displays the scatter distributions among PLS, V_P, L-type SH, and UCS in different rocks.

$$SH(\mathrm{L}) = -2.9154 + 1.1658SH(\mathrm{N}) - 0.0071(SH(\mathrm{N}))^2 + 0.000043(SH(\mathrm{N}))^3 \quad (1)$$

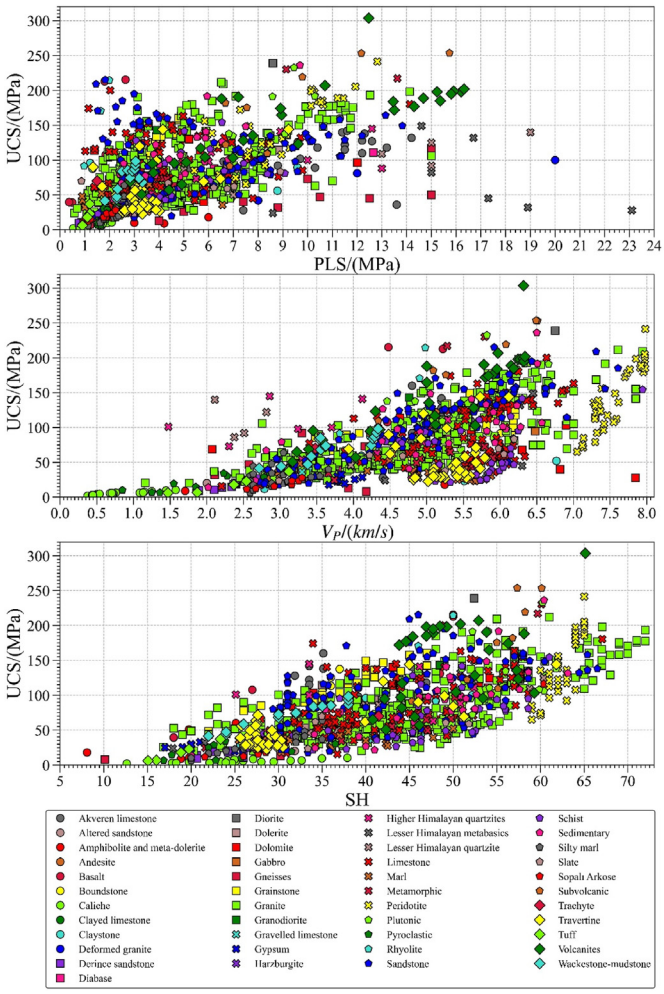

Fig. 2. Scatter distributions among PLS, V_P, SH, and UCS.

2.2. Lithologic classification

Rocks can be categorized into three categories: igneous, sedimentary and metamorphic rocks according to their genesis. Igneous rocks are solidified from molten material known as magma. Sedimentary rocks are formed by the accumulation and cementation of mineral and organic particles. Metamorphic rocks result from the alteration of existing rock (either igneous, sedimentary, or older metamorphic rock) due to heat, pressure, or chemically reactive fluids. Different rocks have different physical and mechanical properties due to their different diagenetic characteristics. For example, igneous rocks are harder and denser compared to other rock types. Sedimentary rocks generally have higher porosity than igneous and metamorphic rocks, and they tend to be less compact and weaker than igneous and metamorphic rocks due to their clastic nature. Metamorphic rocks, undergoing mineralogical and textural changes from their original state, display wide-ranging variations in density and strength. All collected datasets were classified into sedimentary, igneous, and metamorphic rocks based on the distinctive physical and mechanical attributes arising from their individual formation processes. Table 2 lists the classification results of different rocks. There are 494 sedimentary, 494 igneous, and 92 metamorphic samples in the collected datasets. The number of metamorphic rocks is less abundant.

Granite, sandstone, limestone, travertine, schist, and peridotite occupy the largest proportion of all collected datasets. There are 353 granite rock samples in the database. Granite belongs to igneous rock and is a common rock that occurs in quarries, mining, tunnels, slopes, civil

Table 2
Lithologic classification results of different rocks.

No.	Category	Detailed rock type
1	Sedimentary (494)	Akveren limestone (22), Altered sandstone (1), Boundstone (28), Caliche (19), Clayed limestone (1), Claystone (21), Derince sandstone (10), Dolomite (15), Grainstone (28), Gravelled limestone (1), Gypsum (10), Limestone (95), Marl (28), Sandstone (100), Sedimentary (28), Silty marl (26), Sopalı Arkose (8), Travertine (39), and Wackestone-mudstone (14)
2	Igneous (494)	Andesite (1), Basalt (6), Deformed granite (4), Diabase (4), Diorite (1), Dolerite (4), Gabbro (1), Gneisses (12), Granite (353), Granodiorite (1), Harzburgite (1), Peridotite (35), Plutonic (14), Pyroclastic (10), Rhyolite (3), Subvolcanic (8), Trachyte (1), Tuff (5), and Volcanites (30)
3	Metamorphic (92)	Amphibolite and meta-dolerite (5), Higher Himalayan quartzites (12), Lesser Himalayan metabasics (7), Lesser Himalayan quartzite (9), Metamorphic (13), Schist (36), and Slate (10)

construction, etc. Granite has different weathering grades (Ng et al., 2015). Granite rocks with fresh, slightly weathered, and moderately weathered degrees were collected in this study. Sandstone is a typical clastic sedimentary rock composed of various sand cementations. 100 sandstone samples are contained in the database. Limestone (95 samples) is a carbonate sedimentary rock mainly used for concrete aggregates, cement, paving stones, etc. Travertine (39 samples) is a form of terrestrial limestone. Schist (36 samples) is a metamorphic rock with pronounced schistosity. Peridotite (35 samples) is a dense, coarse-grained igneous rock consisting mostly of the silicate minerals olivine and pyroxene. In addition to the rocks described above, some other rocks are also considered, as shown in Table 2.

2.3. Step-by-step study flowchart

The collected datasets consisting of a variety of rocks were divided into three categories, i.e., sedimentary, igneous, and metamorphic rocks, based on lithology. According to Fig. 3, statistical analysis was performed on the collected datasets. The optimal distributions of parameters and the correlation among parameters were determined in different rock types. The tree-based models and linear regression were combined by a stacking strategy to establish stacking models. The stacking models were developed by training datasets and evaluated by testing datasets. Moreover, the validation datasets were employed to compare the advantages of the proposed stacking models. Finally, the sensitivity analysis was conducted for the developed stacking models.

3. Statistical analysis

3.1. Statistical description

Table 3 presents some statistical indicators to describe the PLS, V_P, SH, and UCS in different rocks. According to the mean value, it can be found that igneous rocks have the highest average value of UCS. Metamorphic rocks have the lowest mean value of UCS. Additionally, four parameters in igneous rocks have a large degree of dispersion in terms of standard deviation (Std). Skewness is applied to measure the symmetry of the data distribution. When the distribution is symmetric, the skewness is 0. The skewness of PLS in three types of rock is more than 1, which indicates that the PLS is highly skewed. The correlation coefficient between PLS, V_P, SH, and UCS was calculated for each of three rock types, as depicted in Fig. 4. UCS has the strongest correlation with SH in sedimentary and metamorphic rocks. The strongest correlation is observed between V_P and UCS in igneous rock.

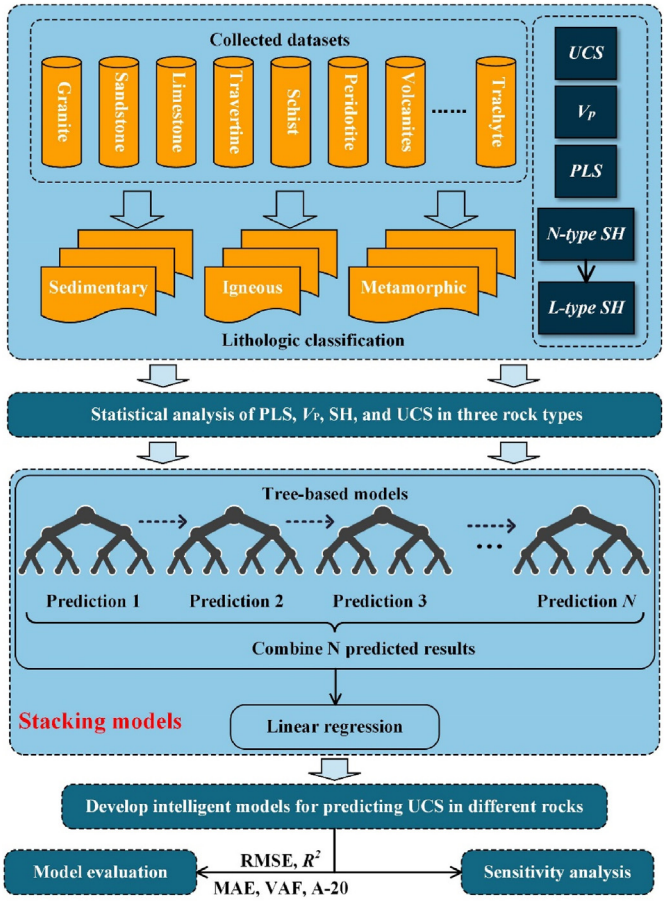

Fig. 3. Technique flowchart of this study.

3.2. Distribution determination

The K–S test was applied to determine the optimal probability distribution satisfying for the PLS, V_P, SH, and UCS in the three rock types. The K–S test is a nonparametric hypothesis test used to determine whether a set of samples is drawn from a specific probability distribution. Normal, log-normal, genlogistic, exponent, right-skewed Gumbel (gumbel_r), and fisk were considered as the potential probability distributions. Eqs. (2)–(7) present the probability density functions of the six candidate distributions. Fig. 5 presents the flowchart to perform the K–S test. First, the null hypothesis (H_0) and the alternative hypothesis (H_1) are established. The distribution function for datasets is chosen. Then, the statistic D is built. When $D < D_{n,\alpha}$, (i.e., p-value $> \alpha$, where α is the significant level), H_0 is accepted. In this study, *Scipy* (Virtanen et al., 2020), a *Python* library, is adopted to perform the K–S test to find the appropriate probability distribution of the PLS, V_P, SH, and UCS in sedimentary, igneous, and metamorphic rocks. *Scipy* can return the statistic D and p-value. The satisfactory probability distribution is determined according to p-value and α. The p-value $> \alpha$ indicates that the samples satisfy the given distribution. A large p-value is accompanied by a great performance of the distribution model.

$$f_{normal}(x) = \frac{\exp(-x^2/2)}{\sqrt{2\pi}} \tag{2}$$

$$f_{\log-normal}(x,c) = \frac{1}{cx\sqrt{2\pi}}\exp\left(-\frac{\log^2(x)}{2c^2}\right) \tag{3}$$

$$f_{genlogistic}(x,c) = c\frac{\exp(-x)}{(1+\exp(-x))^{c+1}} \tag{4}$$

Table 3
Statistical description of four parameters in different rocks.

Indicators	PLS/(MPa)			V_P/(km/s)		
	Metamorphic	Sedimentary	Igneous	Metamorphic	Sedimentary	Igneous
Number	92	494	494	92	494	494
Mean	6.33	4.15	5.42	4.95	4.68	4.96
Std	4.48	2.76	3.34	1.24	1.39	1.39
Min	0.86	0.53	0.36	1.48	0.38	0.85
25%	3.29	2.4	2.99	4.43	3.78	4
50%	4.56	3.27	4.83	5.24	5.05	4.98
75%	7.26	4.96	7.12	5.83	5.67	5.9
Max	23.1	14.2	20	7.94	7.85	7.98
Skewness	1.69	1.5	1.11	−0.94	−0.91	−0.05
Kurtosis	2.48	1.86	1.22	0.68	0.62	−0.13
Indicators	SH			UCS/(MPa)		
	Metamorphic	Sedimentary	Igneous	Metamorphic	Sedimentary	Igneous
Number	92	494	494	92	494	494
Mean	42.12	37.61	45.52	71.37	74.99	92.52
Std	11.69	10.41	12.23	41.84	46.27	53.06
Min	8.08	12.63	10.13	9	2.03	6.2
25%	33.51	30	37.53	41.55	36.31	51.42
50%	45.36	35.44	45.6	62.44	68.06	77.95
75%	50.87	45.37	54	92.45	110.6	123.5
Max	61	67.07	72	230.21	236.19	303.67
Skewness	−0.57	0.5	−0.2	1.29	0.53	0.84
Kurtosis	−0.53	−0.42	−0.39	2.37	−0.41	0.13

Note: 25% represents the 25% quantile, 50% represents the 50% quantile, and 75% represents the 75% quantile.

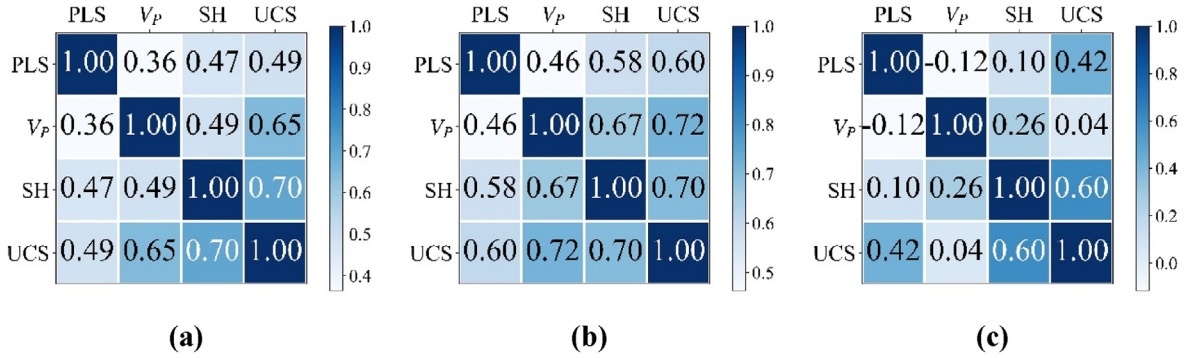

Fig. 4. The correlation among PLS, V_P, SH, and UCS for (a) Sedimentary; (b) Igneous; (c) Metamorphic rocks.

$$f_{\exp\ onent}(x) = \exp(-x) \tag{5}$$

$$f_{gumbel\_r}(x) = \exp(-(x+e^{-x})) \tag{6}$$

$$f_{fisk}(x,c) = \frac{cx^{c-1}}{(1+x^c)^2} \tag{7}$$

where c is the shape parameter.

In this study, α is set to 0.05. The probability distributions with p-values greater than 0.05 are considered. The distribution with the largest p-value is determined to be the optimal distribution. Table 4 presents the optimal distributions of PLS, V_P, SH, and UCS and their corresponding p-values. Fig. 6 displays the probability distribution histogram for PLS, V_P, SH, and UCS in sedimentary, igneous, and metamorphic rocks. The fisk distribution is applicable to the PLS of sedimentary and metamorphic rocks. Most PLS values in sedimentary and metamorphic datasets are skewed towards lower values, with a tail that extends to higher values. The log-normal distribution of PLS in igneous rocks indicates a wide range of PLS values in igneous rocks. The genlogistic distribution for SH across all rock types indicates a wide span of SH values for these rocks. The gumbel_r distribution of UCS in sedimentary rocks suggests a high dominance of low UCS values, with sporadic occurrences of instances with high UCS values. Conversely, the fisk distribution for igneous and metamorphic rocks suggests comparatively uniform UCS values with rare instances of extreme values.

3.3. Simple regression analysis

Simple regression analysis was implemented to describe the relationship between PLS, V_P, SH, and UCS. Three functions, namely linear, exponent, and power, were employed to fit the relationship in PLS-UCS, V_P-UCS, and SH-UCS. The coefficient of determination (R^2) was utilized to evaluate the performances of obtained equations, as shown in Eq. (8). The equation with a larger R^2 was selected. Fig. 7 shows the best-fitted equations in three rock types. R^2 of linear formulas fitted by SH and UCS is the highest in sedimentary rocks, and it is 0.494. R^2 of power formulas fitted by V_P and UCS is the highest in igneous rocks, and it is 0.516. R^2 of exponential formulas fitted by SH and UCS is the highest in metamorphic rocks, and it is 0.38. R^2 is low for the fitted formula between a single variable and UCS in three rock types. This phenomenon indicates that a single parameter is not a strong predictor of UCS in three rocks. Simple regression formulas cannot describe the relationship between PLS, V_P, SH, and UCS. Therefore, further research is needed to employ more powerful modeling techniques for improving the

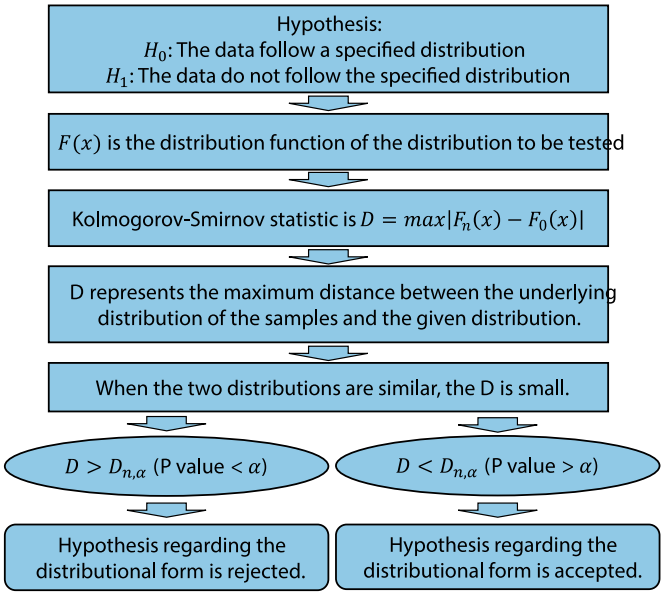

Fig. 5. Flowchart to perform K–S test.

Table 4
Optimal marginal distributions of PLS, V_P, SH, and UCS.

Sedimentary					
Parameter	Distribution	*P*-value	*c*	*loc*	*scale*
PLS	Fisk	0.138	2.551	0.314	3.047
V_P	Genlogistic	0.133	0.232	5.951	0.321
SH	Genlogistic	0.134	11.817	12.686	8.313
UCS	Gumbel_r	0.054		53.136	37.657
Igneous					
Parameters	Distribution	*P*-value	*c*	*loc*	*scale*
PLS	Log-normal	0.678	0.527	−0.87	5.499
V_P	Fisk	0.768	64967183	−51466890	51466895
SH	Genlogistic	0.815	0.849	47.507	6.650
UCS	Fisk	0.236	3.172	−9.196	89.19
Metamorphic					
Parameters	Distribution	*P*-value	*c*	*loc*	*scale*
PLS	Fisk	0.251	2.541	0.512	4.443
V_P	Genlogistic	0.973	0.202	6.082	0.245
SH	Genlogistic	0.539	0.289	52.569	3.393
UCS	Fisk	0.893	3.322	−7.833	70.068

Note: *loc* and *scale* represent shifting and scaling the distribution in *scipy*, respectively.

estimation of UCS according to multiple variables.

Moreover, the R^2 values of PLS-UCS, V_P-UCS, and SH-UCS in metamorphic rocks are notably lower compared to sedimentary and igneous rocks. The low R^2 values are mainly attributed to the data size and data quality of metamorphic rocks. Compared to sedimentary and igneous rocks, the data size of metamorphic rocks is less, and more outliers exist. The limited size of the datasets and the presence of outliers contribute to the lower R^2 values in the fitted equations for metamorphic rocks.

$$R^2 = 1 - \frac{\sum_{i=1}^{n} \left(UCS_i - UCS_{pi}\right)^2}{\sum_{i=1}^{n} \left(UCS_i - \overline{UCS}\right)^2} \tag{8}$$

where UCS_{pi} represents the estimated UCS, $\overline{UCS}$ is the mean of measured UCS, and n is the number of all samples.

4. Predictive model building

4.1. Tree-based models

Tree-based models are introduced to estimate UCS based on the collected databases in different rock types. Tree-based models combine the outputs of multiple regression trees. Four tree-based models are considered in this study. These four tree-based models include adaptive boosting (AdaBoost), gradient boosting machine (GBM), light gradient boosting machine (LightGBM), and RF. These four models are easy to use and less prone to overfitting compared to other tree-based models. Moreover, these four models have good performance on the default hyperparameters. It does not take too much time to tune the hyperparameters of these models. It is easy to use these four tree-based models and other regression models to build ensemble models (Li et al., 2022a).

RF (Breiman, 2001) integrates several regression trees to make predictions. Each tree is built on a random subset of the training data and features. The predictions from all trees are integrated as the final prediction. RF can deal with large datasets, capture non-linear relationships, and reduce variance. However, the development of the RF model is computationally expensive and time-consuming.

AdaBoost (Freund and Schapire, 1997) is a boosting algorithm that focuses on sequentially improving the performance of weak learners. In AdaBoost, a weak learner (regression tree) is initially trained on the original training data. A high weight is assigned to the misclassified instance, and another weak learner is established by the modified data. This process is repeated iteratively, and each subsequent weak learner pays more attention to the previously misclassified instances. AdaBoost is a robust model suited for regression tasks and exhibits flexibility. It can be combined with any regression model. However, AdaBoost is sensitive to noisy data.

GBM (Friedman, 2001) is another boosting method integrating regression trees to create a powerful model. GBM works by iteratively training weak learners on the residuals of the previous learners. In each iteration, the weak learner is trained to minimize the loss function. The final prediction is obtained by aggregating the predictions of all weak learners. GBM does not require excessive data preprocessing, and it is adaptable to various problems. However, GBM often results in a complex ensemble of trees that can be hard to interpret.

LightGBM (Ke et al., 2017) is the variation of gradient boosting that introduces several optimizations to enhance training speed and memory usage. It uses a histogram-based approach to compute the gradients and performs leaf-wise tree growth instead of level-wise (as done by traditional GBM). These optimizations make LightGBM faster and more memory-efficient compared to GBM, especially for large datasets. LightGBM retains the accuracy and flexibility of GBM and is widely used in various applications. However, LightGBM might suffer from overfitting on small datasets.

4.2. Stacking model development

Rock parameter datasets used to develop the predictive model for UCS are usually characterized by both linear and non-linear trends. In this study, previous simple regression analysis also showed that the relationship between PLS, V_P, SH, and UCS presented a mix of linear and non-linear patterns. Tree-based models excel at capturing non-linear relationships between variables. Linear regression can effectively process variables with linear trends. The combination of the tree-based model and linear regression by stacking strategy can combine the advantages of both models, which are suitable for the collected datasets that present both linear and non-linear trends. Therefore, the stacking model combining the tree-based model and linear regression was proposed to predict UCS based on PLS, V_P, and SH. Additionally, the stacking models have greater robustness, which can handle outliers. Furthermore, the stacking model contributes to reducing overfitting, enabling the model to more effectively generalize to new data (Koopialipoor et al., 2022;

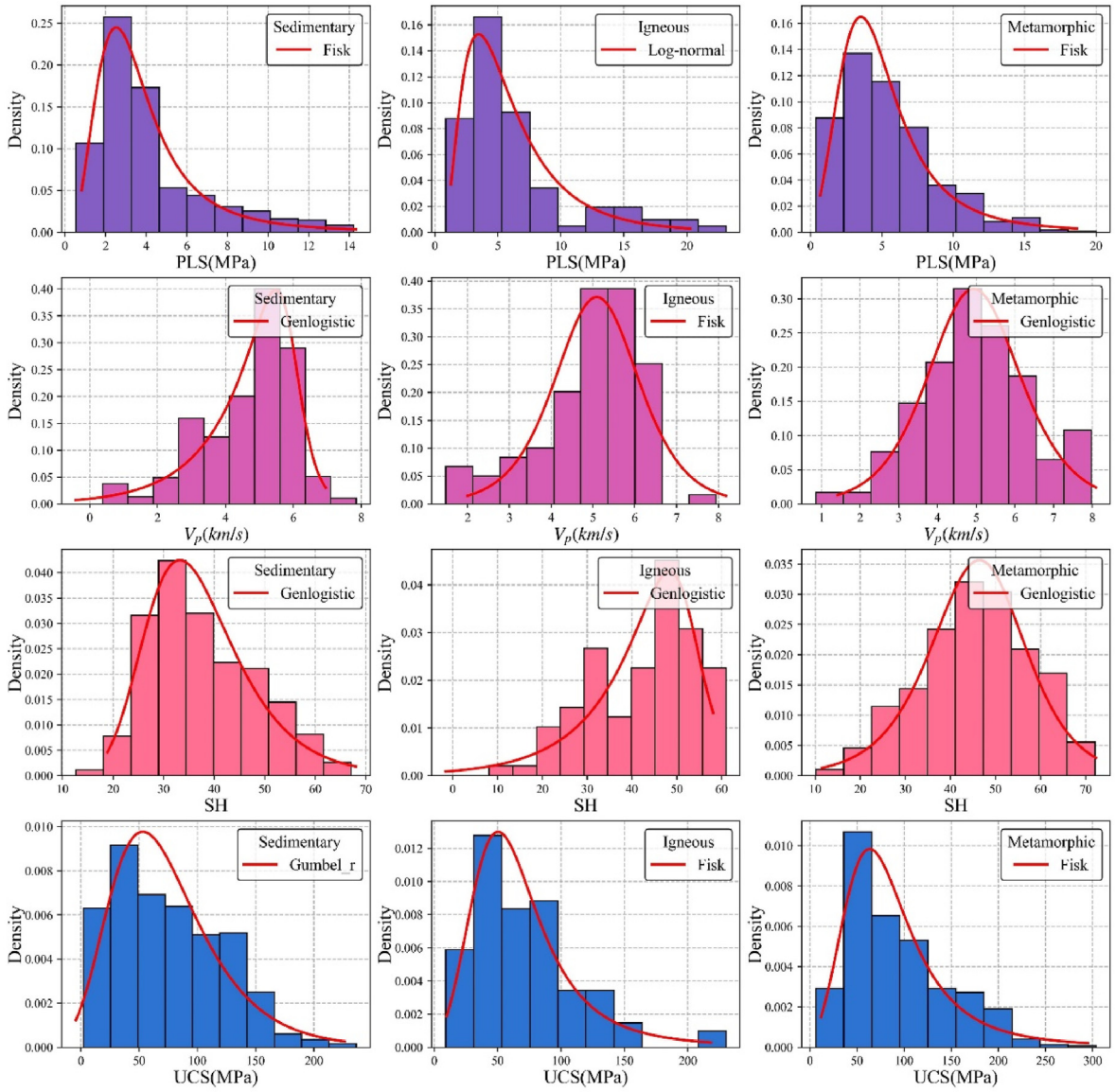

Fig. 6. Probability distributions of four parameters in three rock types.

Pavlyshenko, 2018; Zhou, 2019).

The stacking model is an ensemble learning technique that uses base models to predict output and then employs another model (called meta-model or second-level model) to predict the final output based on the predictions of base models. The basic principle behind stacking is to combine the strengths of different models to improve the final predictive performance. In this study, the tree-based model was used as the base model. Linear regression (LR) was used as the meta-model. Fig. 8 presents the schematic diagram to build the stacking model. Tree-based models are trained using the original training datasets. Once the tree-based models are trained, they output the predicted results of the original training datasets. New datasets are composed of the predicted results by tree-based models and actual UCS values. The LR model is trained based on the new datasets. Stacking models are developed when the training of the tree-based model and LR model is completed. When predicting, the tree-based model first makes a prediction, and then the LR model takes the prediction as input and makes the final prediction. Stacking often leads to better predictive performance compared to individual base models, and it can combine the strengths and mitigate the weaknesses of individual base models. Moreover, stacking can mitigate the overfitting of individual models.

The open-source *Python* library, *Scikit-learn* (Pedregosa et al., 2011), was used to develop the stacking models. The developed stacking models are composed of tree-based models and LR models. LR model does not have hyperparameters to tune. The parameter setting of stacking models is only related to the hyperparameter setting of tree-based models. These four models (RF, AdaBoost, GBM, and LightGBM) have good performance on the default hyperparameters. Therefore, the hyperparameters of tree-based models used the default parameters in *Scikit-learn*. Table 5 shows the key hyperparameters of the four tree-based models. Finally, four stacking models, RF-LR, AdaBoost-LR, GBM-LR, and LightGBM-LR, were constructed.

4.3. Modeling results

R^2, root mean square error (RMSE), mean absolute error (MAE), the variance accounted for (VAF), and the A-20 index are calculated to evaluate the developed models. Eqs. (9)–(12) present these calculation equations. When VAF and A-20 are large, the capability of the developed model is better. Small RMSE and MAE indicate the great capacity of the model.

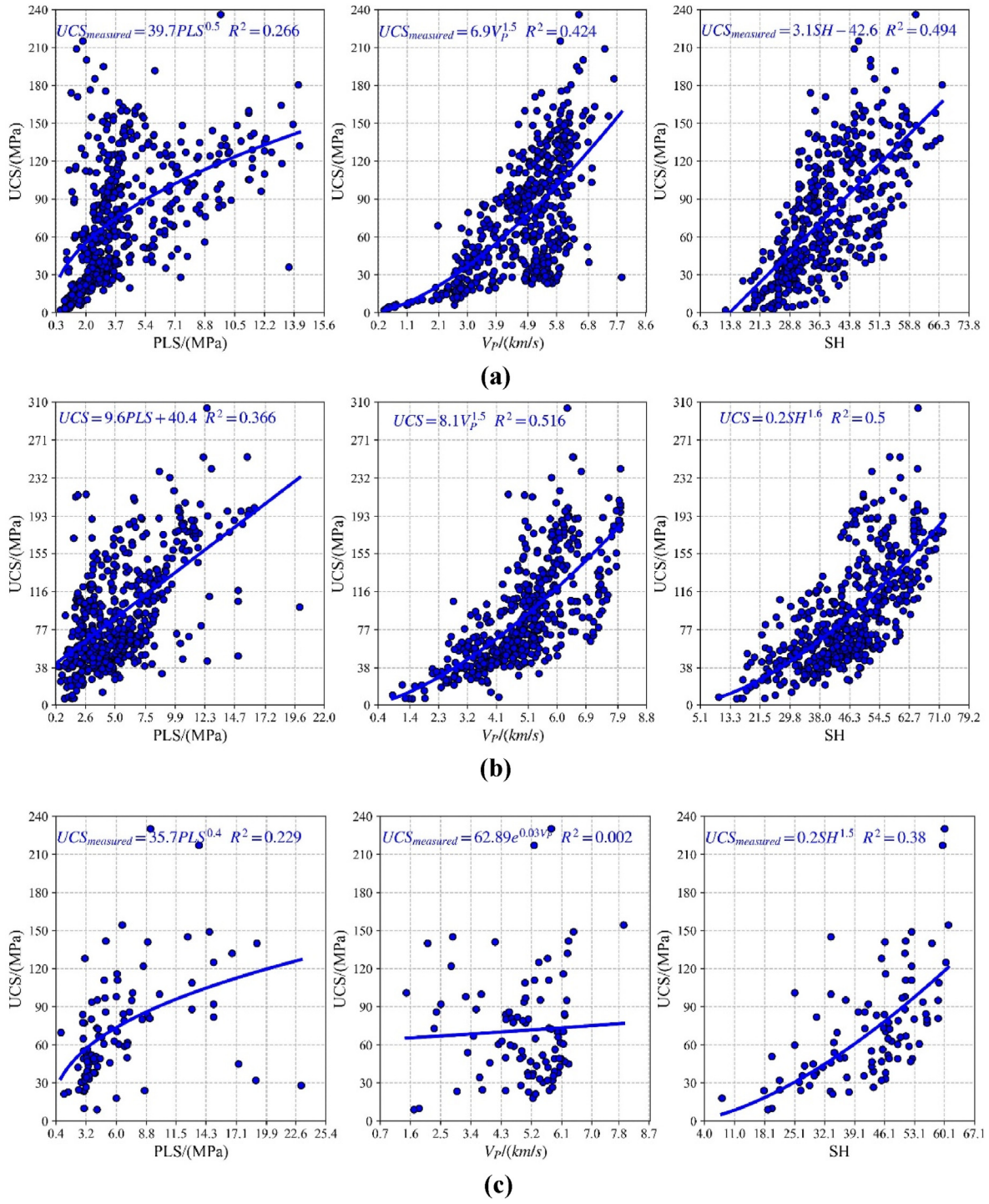

Fig. 7. The best-fitted equations and curves in three rock types: (a) Sedimentary; (b) Igneous; (c) Metamorphic rocks.

$$\mathrm{RMSE}=\sqrt{\frac{1}{n}\sum_{i=1}^{n}\left(UCS_i-UCS_{pi}\right)^2} \tag{9}$$

$$\mathrm{MAE}=\frac{1}{n}\sum_{i=1}^{n}\left|UCS_i-UCS_{pi}\right| \tag{10}$$

$$\mathrm{VAF}=\left[1-\frac{\mathrm{var}\left(UCS_i-UCS_{pi}\right)}{\mathrm{var}\left(UCS_i\right)}\right]\times 100 \tag{11}$$

$$A-20=\frac{m20}{n} \tag{12}$$

where $m20$ depicts the number of samples whose forecasted UCS is between 0.8 and 1.2 times the actual UCS.

Three databases of sedimentary, igneous, and metamorphic rocks were applied to train the proposed stacking models. These databases were divided into two parts, one part (80%) was applied to develop stacking models, and the other (20%) was used to evaluate these models. Eq. (13) was applied to process the input parameters.

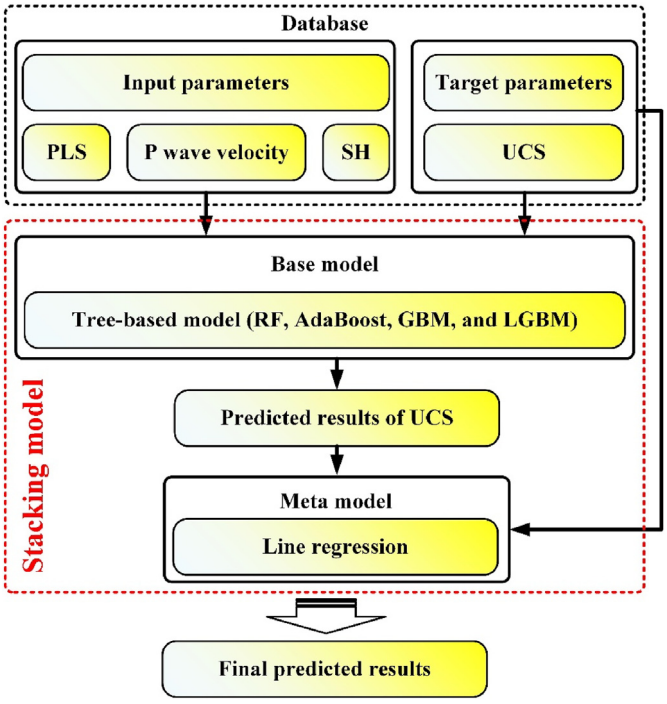

Fig. 8. The schematic diagram to build the stacking model.

Table 5
The hyperparameter value of tree-based models.

Model	Hyperparameter	Value
RF	The number of trees	100
	The minimum sample number of internal nodes for splitting	2
	The minimum sample number of leaf nodes	1
AdaBoost	The number of trees	50
	Learning rate	1
GBM	The number of boosting iterations	100
	Learning rate	0.1
LightGBM	Number of boosted trees	100
	Learning rate	0.1

$$V' = \frac{V - V.mean}{V.std} \tag{13}$$

where *V.mean* stands for the mean of rock parameters, and *V.std* depicts the standard deviation of rock parameters.

Tables 6–8 list the training and testing performances of developed stacking models in sedimentary, igneous, and metamorphic rocks, respectively. Additionally, ranking systems are implemented to select the best model for three rock types. Stacking models are ranked according to their performances in each regression indicator. Great performance is associated with a high rank. The ranks of five regression indicators are summed to get the total rank, as shown in Tables 6–8. Considering the training and testing performances, the total ranks in training and testing sets are summed to obtain the final rank. The model with the highest final rank is the best. Fig. 9 exhibits the final rank of stacking models in three rock types. It can be found that RF-LR performs best in three rock types. Compared to sedimentary and igneous rocks, stacking models developed by metamorphic datasets perform poorly in the testing set due to the small size and quality of data.

5. Discussion

5.1. Model validation and comparison

Four stacking models are developed to predict UCS based on collected databases in sedimentary, igneous, and metamorphic rocks. The best models are determined according to ranking systems. To compare the superiority of the proposed stacking models, datasets including PLS, V_P, SH, and UCS in three rock types are applied to train RF, AdaBoost, GBM, and LightGBM. An additional validation database is collected to compare the capabilities of stacking models and tree-based models. The validation database includes 110 datasets, which are from Armaghani et al. (2015), Güneyli et al. (2022), and Jalali et al. (2017). 50 granite samples, 11 grainstone samples, 21 boundstone samples, 1 gypsum sample, 6 silty marl samples, 11 mudstone samples, 3 metagabbro samples, 1 ophicalcite sample, 5 marble samples, and 1 serpentine sample are compiled. There are 50 igneous, 50 sedimentary, and 10 metamorphic samples in the database. The detailed datasets can be found in the supplement.

Fig. 10 shows the validation performances (R^2) of stacking models and tree-based models in sedimentary, igneous, and metamorphic rocks, respectively. For sedimentary rocks, the stacking models have the same performance as the tree-based models. Even the performances of RF-LR and LightGBM-RF are worse than those of RF and LightGBM. For igneous rocks, except for AdaBoost-LR, the other stacking models perform better than their base models (RF, GBM, and LightGBM). For metamorphic rocks, all stacking models perform better than tree-based models. This suggests that the combination of tree-based models and linear regression by stacking strategy can significantly improve the performances of the tree-based models, which are beneficial to estimating the UCS of metamorphic rocks. Overall, the stacking models proposed in this study are helpful to predict the UCS of metamorphic and igneous rocks, and the tree-based models are more suitable for the evaluation of UCS in sedimentary rocks.

Uncertainty analysis is conducted on the developed stacking models and tree-based models to estimate their uncertainty for estimating UCS. Firstly, the error of each dataset (e_i) is computed (Eq. (14)). After that, the mean error ($\overline{e}$) and deviation of the error (S_e) are calculated, as shown in Eqs. (15) and (16). $\overline{e} > 0$ suggests the overestimation of the stacking model, and $\overline{e} < 0$ implies the underestimation of the stacking model. A Large S_e is accompanied by a large discreteness of errors, which increases

Table 6
Ranking system to compare the capabilities of stacking model in sedimentary rocks.

Model	R^2		MAE		RMSE		VAF		A-20		Total rank
	Value	Rank	Value	Rank	Value	Rank	Value	Rank	Value	Rank	
Training											
RF-LR	0.93	4	9.575	4	12.35	4	93.505	4	0.669	4	20
AdaBoost-LR	0.71	1	21.16	1	25.106	1	71.3	1	0.351	1	5
GBM-LR	0.863	2	13.91	2	17.24	2	86.806	2	0.553	2	10
LightGBM-LR	0.883	3	12.101	3	15.974	3	88.768	3	0.616	3	15
Testing											
RF-LR	0.816	4	15.036	4	19.148	4	82.166	4	0.541	4	20
AdaBoost-LR	0.704	1	19.976	1	24.304	1	70.381	1	0.367	1	5
GBM-LR	0.795	3	15.805	3	20.209	3	79.62	3	0.51	3	15
LightGBM-LR	0.774	2	17.077	2	21.234	2	77.693	2	0.49	2	10

Table 7
Ranking system to compare the capabilities of stacking model in igneous rocks.

Model	R^2		MAE		RMSE		VAF		A-20		Total rank
	Value	Rank	Value	Rank	Value	Rank	Value	Rank	Value	Rank	
Training											
RF-LR	0.952	4	9.282	4	11.731	4	95.472	4	0.821	4	20
AdaBoost-LR	0.764	1	21.198	1	26.014	1	77.246	1	0.457	1	5
GBM-LR	0.875	2	15.273	2	18.91	2	87.74	2	0.586	2	10
LightGBM-LR	0.888	3	13.655	3	17.944	3	89.159	3	0.684	3	15
Testing											
RF-LR	0.794	4	18.585	3	22.991	4	81.495	4	0.469	1	16
AdaBoost-LR	0.728	2	21.317	1	26.464	1	75.452	1	0.48	2	7
GBM-LR	0.791	3	18.889	2	23.179	2	80.42	2	0.49	3	12
LightGBM-LR	0.794	4	18.397	4	23	3	81.009	3	0.541	4	18

Table 8
Ranking system to compare the capabilities of stacking model in metamorphic rocks.

Model	R^2		MAE		RMSE		VAF		A-20		Total rank
	Value	Rank	Value	Rank	Value	Rank	Value	Rank	Value	Rank	
Training											
RF-LR	0.808	4	13.031	4	17.916	4	80.791	4	0.575	4	20
AdaBoost-LR	0.664	2	19.338	1	23.683	2	66.506	2	0.397	1	8
GBM-LR	0.791	3	14.508	3	18.664	3	79.149	3	0.548	3	15
LightGBM-LR	0.64	1	18.172	2	24.52	1	64.021	1	0.479	2	7
Testing											
RF-LR	0.629	4	20.278	4	26.687	4	63.657	4	0.368	4	20
AdaBoost-LR	0.458	2	23.263	2	32.243	2	46.733	2	0.316	3	11
GBM-LR	0.515	3	22.933	3	30.508	3	51.801	3	0.368	4	16
LightGBM-LR	0.308	1	26.684	1	36.428	1	30.94	1	0.368	4	8

the uncertainty of the model. Additionally, $1.96S_e$ is considered as the 95% confidence interval, representing the width of uncertainty band (Jamei et al., 2021).

$$e_i = UCS_i - UCS_{pi} \tag{14}$$

$$\overline{e} = \sum_{i=1}^{n} e_i \tag{15}$$

$$S_e = \sqrt{\frac{\sum_{i=1}^{n} (e_i - \overline{e})^2}{n-1}} \tag{16}$$

Fig. 11 exhibits $\overline{e}$, S_e, and width of uncertainty band of stacking models and tree-based models in different rock types. The UCS values of metamorphic rocks tend to be overestimated by these models. The absolute values of $\overline{e}$ in metamorphic rocks are larger than those of other rock types, and UCS values of metamorphic rocks are less predictable than those of other rock types. The stacking models have less absolute values of $\overline{e}$ in metamorphic rocks compared to tree-based models. This suggests that the stacking models can reduce the predicted error and improve predictive performance for UCS of metamorphic rocks. The models developed by igneous rocks have the largest uncertainty, which is due to the wide range distribution of UCS values of igneous rocks, as shown in Table 3. The RF-LR models in igneous and metamorphic rocks and the RF model in metamorphic rocks have lower uncertainty in terms of the width of the uncertainty band, and they are suitable for the estimation of UCS.

5.2. Significance analysis of parameters

PLS, V_P, and SH are easily obtained, and they are widely utilized to evaluate the UCS of rocks indirectly. In different lithologies, the correlation between these three parameters and UCS is different. Therefore, it is necessary to study key variables for the estimation of UCS in different rock types. The permutation feature importance algorithm (PFIA) is implemented to compute the importance of PLS, V_P, and SH in four stacking models. The mean importance values of PLS, V_P, and SH in four stacking models are calculated. Fig. 12 presents the important scores of input parameters in stacking models for sedimentary, igneous, and metamorphic rocks. In the developed models, SH has more contribution for the evaluation of UCS in sedimentary and metamorphic rocks compared to PLS and V_P. V_P has more contribution for the estimation of UCS in igneous rocks compared to SH and PLS.

SH has a highly important score among the three types of rocks. The Schmidt rebound value measures the rebound hardness of the rock surface. The Schmidt rebound value is not sensitive to the inherent properties of rock, such as saturation, porosity, and microfractures (Buyuksagis and Goktan, 2007), which can be an excellent proxy for the overall strength and hardness of rocks. SH can provide the direct and reliable estimation of UCS in three rock types.

Igneous rocks form from the solidification of magma or lava, resulting in tightly packed crystalline grains that contribute to their high density. Igneous rocks often contain harder minerals, such as quartz and feldspar, which further increase their overall hardness. Compared to other types of rocks, igneous rocks (such as granite and peridotite) are characterized by being harder and denser. Moreover, V_P represents the speed at which compression waves travel through the rock material. The propagation of compression waves in rocks is related to the density and elastic properties of rocks. As such, V_P can offer valuable insights into the structures and properties of igneous rocks, which makes it a valid parameter for estimating UCS in igneous rocks.

Metamorphic rocks are formed through the transformation of other rocks under extreme heat and pressure. The transformation process involves extreme heat and pressure that significantly alters the mineral composition and structure of the parent rock. However, it is important to note that metamorphic processes can lead to an enormous variety in the characteristics of the resulting rock. The variations may result in different relationships between V_P and UCS within various metamorphic rocks, as shown in Fig. 13. There is no consistent relationship between V_P and UCS for all metamorphic rock samples, which causes the V_P to be not a valid variable for UCS prediction compared to PLS and SH.

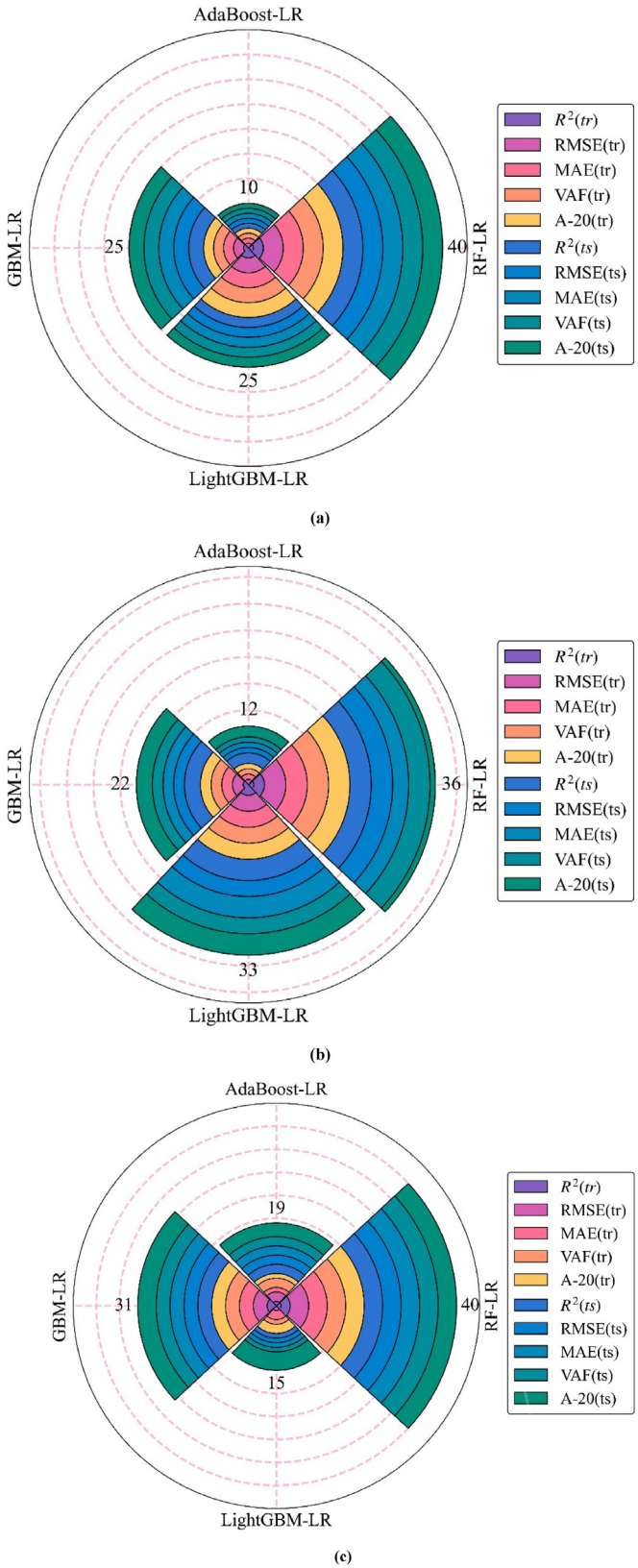

Fig. 9. Final rank of stacking models in three rock types: (a) Sedimentary; (b) Igneous; (c) Metamorphic rocks.

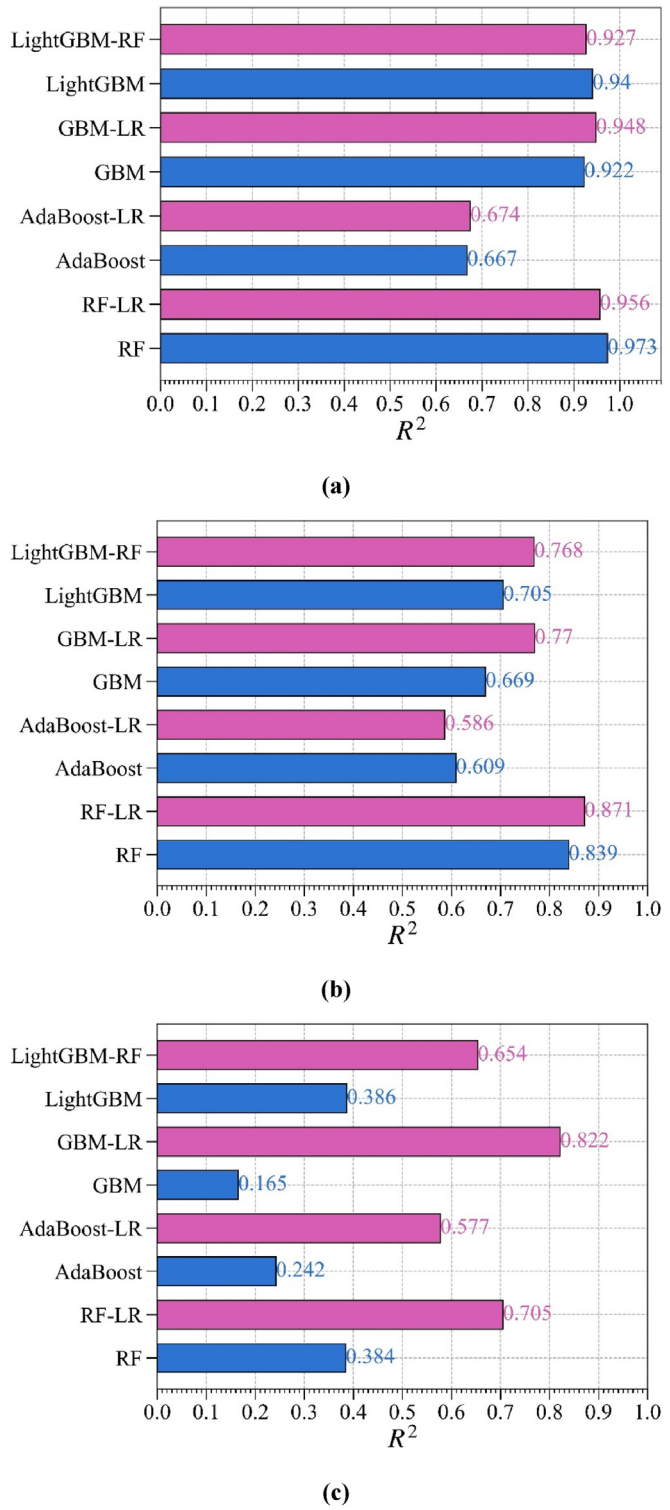

Fig. 10. The validating performance of stacking models and tree-based models: (a) Sedimentary; (b) Igneous; (c) Metamorphic rocks.

The point load test is an effective method to measure the strength of rocks. PLS is directly related to the UCS, and they have the same unit dimension. However, for the developed stacking models, the contribution of PLS to the prediction of UCS is smaller than that of SH and V_P in igneous and sedimentary rocks. This phenomenon is attributed to the dispersion of the collected datasets. In different works of literature, the relationship between PLS and UCS is different, as shown in Figs. 14 and 15. Taking igneous rock as an example, in the collected datasets from

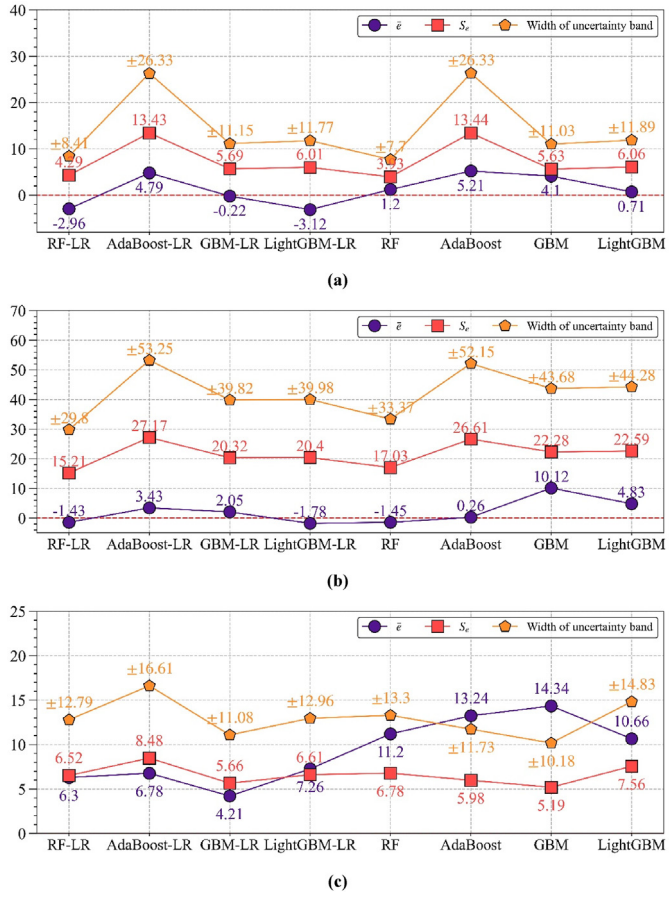

Fig. 11. Uncertainty analysis of stacking models for the estimation of UCS: (a) Sedimentary; (b) Igneous; (c) Metamorphic rocks.

Kallu and Roghanchi (2015), the relationship between UCS and PLS was found to be represented by the equation UCS = 86.9 PLS + 8.9. Conversely, the datasets from Tandon and Gupta (2015) yielded a different formula for UCS, specifically UCS = 4.63 PLS + 12.6. The predictive models developed by these collected databases are influenced by the dispersion of the data, with PLS showing less significance compared to V_P and SH. However, PLS is still an important indicator for evaluating UCS in geotechnical engineering.

6. Limitations and future works

One thousand eighty datasets consisting of PLS, V_P, SH, and UCS were collected and integrated into three categories according to the lithologic character. Stacking models based on tree-based models and linear regression were developed by the collected datasets to estimate UCS in sedimentary, igneous, and metamorphic rocks. The utilization of a stacking strategy, combining tree-based models and linear regression, exhibits significant improvement in predicting the UCS of metamorphic rocks. However, since the datasets were collected from other literature, the sources of the outliers and dispersion of the datasets were unknown. Therefore, there is no way to deal with outliers and discreteness of data. Additionally, the size of the collected metamorphic database is small, and the mechanical properties of different metamorphic rocks are different. Compared to sedimentary and igneous rocks, the predictive models of UCS in metamorphic rocks are misleading because the data quality is not good enough. The stacking models in metamorphic rocks have poor performances during the testing phase. In the future, increasing the data size of metamorphic rock will be conducive to the development of the stacking models. Finally, dividing rock into more detailed categories

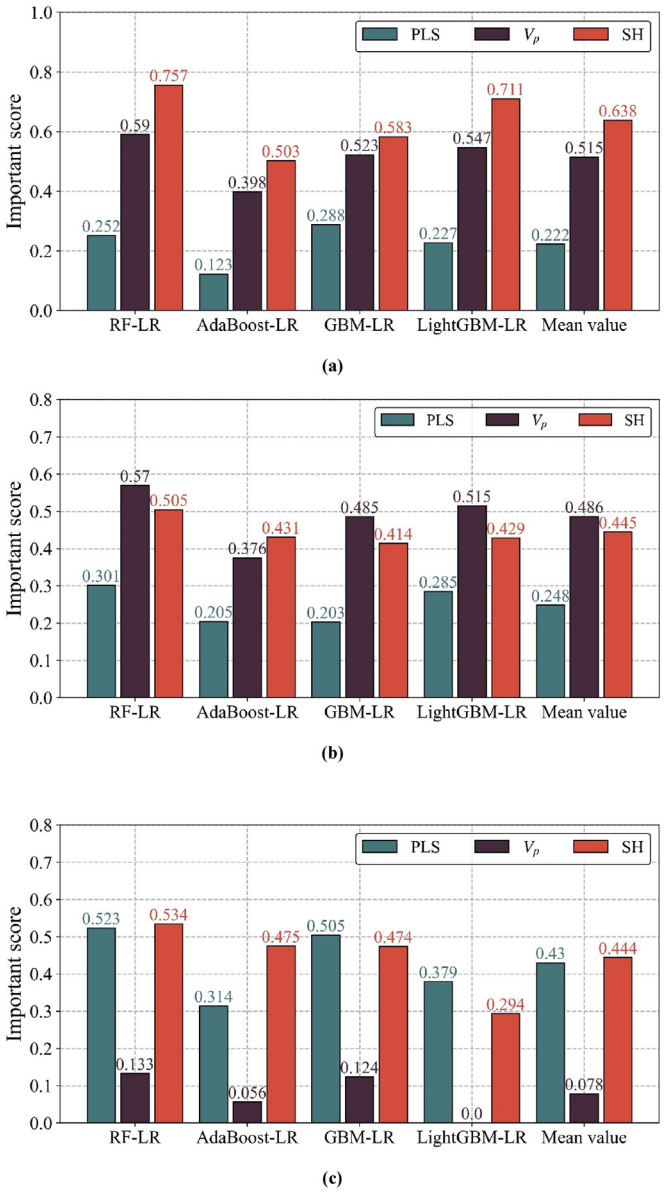

Fig. 12. Important scores of input parameters for estimation of UCS: (a) Sedimentary; (b) Igneous; (c) Metamorphic rocks.

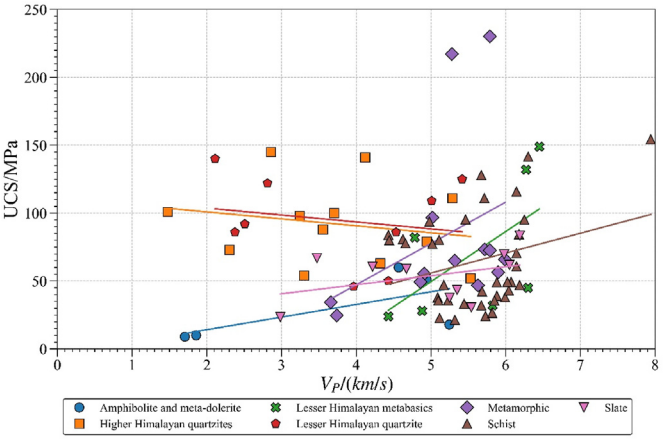

Fig. 13. The relationship between V_P and UCS in different metamorphic rocks.

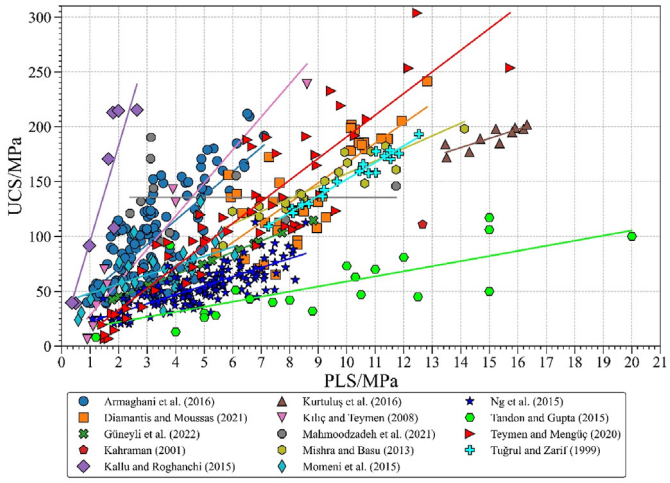

Fig. 14. The relationship between PLS and UCS in igneous rocks from different sources of literature.

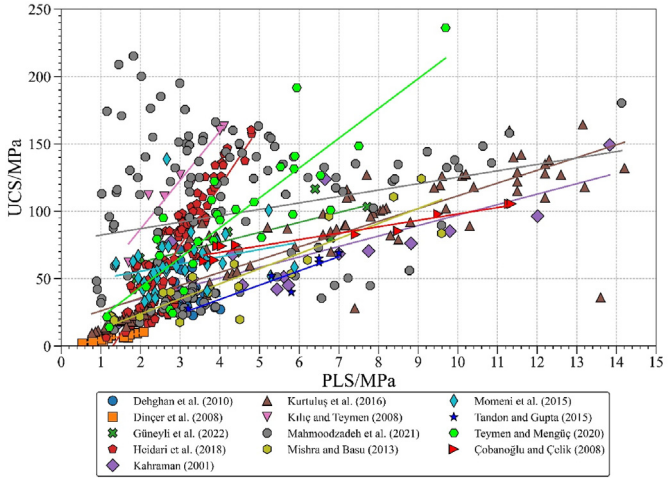

Fig. 15. The relationship between PLS and UCS in sedimentary rocks from different sources of literature.

(such as sandstone, granite, etc.) is more suitable for some actual projects.

7. Conclusions

(1) One thousand eighty datasets were collected and classified into sedimentary, igneous, and metamorphic rocks according to lithology. K–S test determined the optimal distributions for PLS, V_P, SH, and UCS in three rock types, which can be used for geotechnical reliability analysis. Simple regression analysis determined the relationship between PLS, V_P, SH, and UCS in three rock types. The analysis results revealed the underlying dependencies between PLS, V_P, SH, and UCS in three rock types. Additionally, the collected datasets can be used as a substantial resource to build a predictive model of UCS according to engineering needs in the future.

(2) Stacking models based on tree-based models and LR were proposed to predict UCS in different rock types. The RF-LR model is the most optimal stacking model for UCS estimation in three rock types. Model validation shows that the stacking models exhibit superior performance in predicting UCS in metamorphic and igneous rocks, while tree-based models show better suitability for sedimentary rocks. The developed predictive models can be employed to estimate UCS on site, which contributes to the rapid classification of the engineering rock masses.

(3) The contributions of PLS, V_P, and SH for the estimation of UCS were analyzed across different rock types. SH is a valid parameter in predicting UCS across all rock types, particularly in sedimentary and metamorphic rocks. V_P can be used as an indicator to evaluate the UCS of igneous rocks due to its effectiveness and simplicity of the testing procedure. However, V_P is not a reliable variable to evaluate the UCS of metamorphic rocks. This phenomenon is mainly due to the large difference in the properties of different metamorphic rocks, which leads to an inconsistent relationship between V_P and UCS of different metamorphic rocks.

Declaration of interests

The authors declare that they have no known competing financial interests or personal relationships that could have appeared to influence the work reported in this paper.

Acknowledgments

This research was financially supported by the National Natural Science Foundation of China (No. 52374153 and No. 52074349) and the Fundamental Research Funds for the Central Universities of Central South University (No. 2023zzts0726).

Appendix A. Supplementary data

Supplementary data to this article can be found online at https://doi.org/10.1016/j.rockmb.2023.100081.

References

Abdelhedi, M., Jabbar, R., Said, A.B., Fetais, N., Abbes, C., 2023. Machine learning for prediction of the uniaxial compressive strength within carbonate rocks. Earth Sci. Infor. 16 (2), 1473–1487.

Aladejare, A.E., Alofe, E.D., Onifade, M., Lawal, A.I., Ozoji, T.M., Zhang, Z.-X., 2021. Empirical estimation of uniaxial compressive strength of rock: database of simple, multiple, and artificial intelligence-based regressions. Geotech. Geol. Eng. 39, 4427–4455.

Aliyu, M.M., Shang, J., Murphy, W., Lawrence, J.A., Collier, R., Kong, F., Zhao, Z., 2019. Assessing the uniaxial compressive strength of extremely hard cryptocrystalline flint. Int. J. Rock Mech. Min. Sci. 113, 310–321.

Armaghani, D.J., Amin, M.F.M., Yagiz, S., Faradonbeh, R.S., Abdullah, R.A., 2016a. Prediction of the uniaxial compressive strength of sandstone using various modeling techniques. Int. J. Rock Mech. Min. Sci. 85, 174–186.

Armaghani, D.J., Mohamad, E.T., Hajihassani, M., Yagiz, S., Motaghedi, H., 2016b. Application of several non-linear prediction tools for estimating uniaxial compressive strength of granitic rocks and comparison of their performances. Eng. Comput. 32 (2), 189–206.

Armaghani, D.J., Tonnizam Mohamad, E., Momeni, E., Monjezi, M., Sundaram Narayanasamy, M., 2015. Prediction of the strength and elasticity modulus of granite through an expert artificial neural network. Arabian J. Geosci. 9 (1), 48.

Asteris, P.G., Mamou, A., Hajihassani, M., Hasanipanah, M., Koopialipoor, M., Le, T.-T., Kardani, N., Armaghani, D.J., 2021. Soft computing based closed form equations correlating L and N-type Schmidt hammer rebound numbers of rocks. Transport. Geotech. 29, 100588.

Barham, W.S., Rabab'ah, S.R., Aldeeky, H.H., Al Hattamleh, O.H., 2020. Mechanical and physical based artificial neural network models for the prediction of the unconfined compressive strength of rock. Geotech. Geol. Eng. 38 (5), 4779–4792.

Barzegar, R., Sattarpour, M., Deo, R., Fijani, E., Adamowski, J., 2020. An ensemble tree-based machine learning model for predicting the uniaxial compressive strength of travertine rocks. Neural Comput. Appl. 32 (13), 9065–9080.

Bieniawski, Z.T., 1974. Estimating the strength of rock materials. J. S. Afr. Inst. Min. Metall 74 (8), 312–320.

Breiman, L., 2001. Random forests. Mach. Learn. 45 (1), 5–32.

Buyuksagis, I.S., Goktan, R.M., 2007. The effect of Schmidt hammer type on uniaxial compressive strength prediction of rock. Int. J. Rock Mech. Min. Sci. 44 (2), 299–307.

Cao, J., Gao, J., Rad, H.N., Mohammed, A.S., Hasanipanah, M., Zhou, J., 2022. A novel systematic and evolved approach based on XGBoost-firefly algorithm to predict Young's modulus and unconfined compressive strength of rock. Eng. Comput. 38 (5), 3829–3845.

Çobanoğlu, İ., Çelik, S.B., 2008. Estimation of uniaxial compressive strength from point load strength, Schmidt hardness and P-wave velocity. Bull. Eng. Geol. Environ. 67 (4), 491–498.

Corkum, A., Asiri, Y., El Naggar, H., Kinakin, D., 2018. The Leeb hardness test for rock: an updated methodology and UCS correlation. Rock Mech. Rock Eng. 51 (3), 665–675.
Dehghan, S., Sattari, G., Chelgani, S.C., Aliabadi, M., 2010. Prediction of uniaxial compressive strength and modulus of elasticity for Travertine samples using regression and artificial neural networks. Min. Sci. Technol. 20 (1), 41–46.
Diamantis, K., Moussas, V.C., 2021. Estimating uniaxial compressive strength of peridotites from simple tests using neural networks. Arabian J. Geosci. 14 (23), 2690.
Dinçer, İ., Acar, A., Ural, S., 2008. Estimation of strength and deformation properties of Quaternary caliche deposits. Bull. Eng. Geol. Environ. 67 (3), 353–366.
Ebdali, M., Khorasani, E., Salehin, S., 2020. A comparative study of various hybrid neural networks and regression analysis to predict unconfined compressive strength of travertine. Innov. Infrastruct. Sol. 5 (3), 1–14.
Fereidooni, D., 2016. Determination of the geotechnical characteristics of hornfelsic rocks with a particular emphasis on the correlation between physical and mechanical properties. Rock Mech. Rock Eng. 49 (7), 2595–2608.
Freund, Y., Schapire, R.E., 1997. A decision-theoretic generalization of on-line learning and an application to boosting. J. Comput. Syst. Sci. 55 (1), 119–139.
Friedman, J.H., 2001. Greedy function approximation: a gradient boosting machine. Ann. Stat. 29 (5), 1189–1232.
Gowida, A., Elkatatny, S., Gamal, H., 2021. Unconfined compressive strength (UCS) prediction in real-time while drilling using artificial intelligence tools. Neural Comput. Appl. 33, 8043–8054.
Güneyli, H., Güneyli, A., Yapıcı, N., Karahan, S., 2022. Prediction the micro-Deval abrasion loss of rock aggregates from mainly the ultrasonic pulse velocity and some strength parameters. Arabian J. Geosci. 15 (6), 527.
Hatheway, A.W., 2009. The complete ISRM suggested methods for rock characterization, testing and monitoring; 1974–2006. Environ. Eng. Geosci. 15 (1), 47–48.
Heidari, M., Mohseni, H., Jalali, S.H., 2018. Prediction of uniaxial compressive strength of some sedimentary rocks by fuzzy and regression models. Geotech. Geol. Eng. 36 (1), 401–412.
Hoek, E., Carranza-Torres, C., Corkum, B., 2002. *Hoek-Brown Failure Criterion-2002 Edition* Proceedings of NARMS-Tac.
Jalali, S.H., Heidari, M., Mohseni, H., 2017. Comparison of models for estimating uniaxial compressive strength of some sedimentary rocks from Qom Formation. Environ. Earth Sci. 76 (22), 753.
Jamei, M., Hasanipanah, M., Karbasi, M., Ahmadianfar, I., Taherifar, S., 2021. Prediction of flyrock induced by mine blasting using a novel kernel-based extreme learning machine. J. Rock Mech. Geotech. Eng. 13 (6), 1438–1451.
Jin, X., Zhao, R., Ma, Y., 2022. Application of a hybrid machine learning model for the prediction of compressive strength and elastic modulus of rocks. Minerals 12 (12), 1506.
Jing, H., Nikafshan Rad, H., Hasanipanah, M., Jahed Armaghani, D., Qasem, S.N., 2021. Design and implementation of a new tuned hybrid intelligent model to predict the uniaxial compressive strength of the rock using SFS-ANFIS. Eng. Comput. 37 (4), 2717–2734.
Kahraman, S., 2001. Evaluation of simple methods for assessing the uniaxial compressive strength of rock. Int. J. Rock Mech. Min. Sci. 38 (7), 981–994.
Kallu, R., Roghanchi, P., 2015. Correlations between direct and indirect strength test methods. Int. J. Min. Sci. Technol. 25 (3), 355–360.
Ke, G., Meng, Q., Finley, T., Wang, T., Chen, W., Ma, W., Ye, Q., Liu, T.-Y., 2017. Lightgbm: a highly efficient gradient boosting decision tree. Adv. Neural Inf. Process. Syst. 30, 3146–3154.
Kılıç, A., Teymen, A., 2008. Determination of mechanical properties of rocks using simple methods. Bull. Eng. Geol. Environ. 67 (2), 237–244.
Koopialipoor, M., Asteris, P.G., Salih Mohammed, A., Alexakis, D.E., Mamou, A., Armaghani, D.J., 2022. Introducing stacking machine learning approaches for the prediction of rock deformation. Transport. Geotech. 34, 100756.
Kurtuluş, C., Sertçelik, F., Sertçelik, I., 2016. Correlating physico-mechanical properties of intact rocks with P-wave velocity. Acta Geodaetica et Geophysica 51 (3), 571–582.
Li, D., Liu, Z., Armaghani, D.J., Xiao, P., Zhou, J., 2022a. Novel ensemble intelligence methodologies for rockburst assessment in complex and variable environments. Sci. Rep. 12 (1), 1844.
Li, J., Li, C., Zhang, S., 2022b. Application of six metaheuristic optimization algorithms and random forest in the uniaxial compressive strength of rock prediction. Appl. Soft Comput. 131, 109729.
Mahmoodzadeh, A., Mohammadi, M., Ghafoor Salim, S., Farid Hama Ali, H., Hashim Ibrahim, H., Nariman Abdulhamid, S., Nejati, H.R., Rashidi, S., 2022. Machine Learning Techniques to Predict Rock Strength Parameters. Rock Mech. Rock Eng, 55 (3): 1721-1741.
Mahmoodzadeh, A., Mohammadi, M., Ibrahim, H.H., Abdulhamid, S.N., Salim, S.G., Ali, H.F.H., Majeed, M.K., 2021. Artificial intelligence forecasting models of uniaxial compressive strength. Transport. Geotech. 27, 100499.
Miah, M.I., Ahmed, S., Zendehboudi, S., Butt, S., 2020. Machine learning approach to model rock strength: prediction and variable selection with aid of log data. Rock Mech. Rock Eng. 53 (10), 4691–4715.
Mishra, D., Basu, A., 2013. Estimation of uniaxial compressive strength of rock materials by index tests using regression analysis and fuzzy inference system. Eng. Geol. 160, 54–68.
Momeni, E., Jahed Armaghani, D., Hajihassani, M., Mohd Amin, M.F., 2015. Prediction of uniaxial compressive strength of rock samples using hybrid particle swarm optimization-based artificial neural networks. Measurement 60, 50–63.
Moussas, V.C., Diamantis, K., 2021. Predicting uniaxial compressive strength of serpentinites through physical, dynamic and mechanical properties using neural networks. J. Rock Mech. Geotech. Eng. 13 (1), 167–175.
Najibi, A.R., Ghafoori, M., Lashkaripour, G.R., Asef, M.R., 2015. Empirical relations between strength and static and dynamic elastic properties of Asmari and Sarvak limestones, two main oil reservoirs in Iran. J. Petrol. Sci. Eng. 126, 78–82.
Ng, I.-T., Yuen, K.-V., Lau, C.-H., 2015. Predictive model for uniaxial compressive strength for Grade III granitic rocks from Macao. Eng. Geol. 199, 28–37.
Özdemir, E., 2022. A new predictive model for uniaxial compressive strength of rock using machine learning method: artificial intelligence-based age-layered population structure genetic programming (ALPS-GP). Arabian J. Sci. Eng. 47, 629–639.
Palmström, A., 1996. Characterizing rock masses by the RMi for use in practical rock engineering: Part 1: the development of the Rock Mass index (RMi). Tunn. Undergr. Space Technol. 11 (2), 175–188.
Parsajoo, M., Armaghani, D.J., Mohammed, A.S., Khari, M., Jahandari, S., 2021. Tensile strength prediction of rock material using non-destructive tests: a comparative intelligent study. Transport. Geotech. 31, 100652.
Pavlyshenko, B., 2018. Using stacking approaches for machine learning models, 21-25 Aug. 2018. In: 2018 IEEE Second International Conference on Data Stream Mining & Processing (DSMP).
Pedregosa, F., Varoquaux, G., Gramfort, A., Michel, V., Thirion, B., Grisel, O., Blondel, M., Prettenhofer, P., Weiss, R., Dubourg, V., 2011. Scikit-learn: machine learning in Python. J. Mach. Learn. Res. 12, 2825–2830.
Rahman, T., Sarkar, K., 2021. Lithological control on the estimation of uniaxial compressive strength by the P-wave velocity using supervised and unsupervised learning. Rock Mech. Rock Eng. 54 (6), 3175–3191.
Shahri, A.A., Moud, F.M., Lialestani, S.P.M., 2022. A hybrid computing model to predict rock strength index properties using support vector regression. Eng. Comput. 38, 579–594.
Sharma, L., Vishal, V., Singh, T., 2017. Developing novel models using neural networks and fuzzy systems for the prediction of strength of rocks from key geomechanical properties. Measurement 102, 158–169.
Sun, H., Du, W., Liu, C., 2021. Uniaxial compressive strength determination of rocks using X-ray computed tomography and convolutional neural networks. Rock Mech. Rock Eng. 54, 4225–4237.
Tandon, R.S., Gupta, V., 2015. Estimation of strength characteristics of different Himalayan rocks from Schmidt hammer rebound, point load index, and compressional wave velocity. Bull. Eng. Geol. Environ. 74 (2), 521–533.
Teymen, A., Mengüç, E.C., 2020. Comparative evaluation of different statistical tools for the prediction of uniaxial compressive strength of rocks. Int. J. Min. Sci. Technol. 30 (6), 785–797.
Török, Á., Vásárhelyi, B., 2010. The influence of fabric and water content on selected rock mechanical parameters of travertine, examples from Hungary. Eng. Geol. 115 (3–4), 237–245.
Tuğrul, A., Zarif, I., 1999. Correlation of mineralogical and textural characteristics with engineering properties of selected granitic rocks from Turkey. Eng. Geol. 51 (4), 303–317.
Uyanık, O., Sabbağ, N., Uyanık, N.A., Öncü, Z., 2019. Prediction of mechanical and physical properties of some sedimentary rocks from ultrasonic velocities. Bull. Eng. Geol. Environ. 78 (8), 6003–6016.
Virtanen, P., Gommers, R., Oliphant, T.E., Haberland, M., Reddy, T., Cournapeau, D., Burovski, E., Peterson, P., Weckesser, W., Bright, J., van der Walt, S.J., Brett, M., Wilson, J., Millman, K.J., Mayorov, N., Nelson, A.R.J., Jones, E., Kern, R., Larson, E., Carey, C.J., Polat, İ., Feng, Y., Moore, E.W., VanderPlas, J., Laxalde, D., Perktold, J., Cimrman, R., Henriksen, I., Quintero, E.A., Harris, C.R., Archibald, A.M., Ribeiro, A.H., Pedregosa, F., van Mulbregt, P., Contributors, S., 2020. SciPy 1.0: fundamental algorithms for scientific computing in Python. Nat. Methods 17, 261–272.
Wang, M., Wan, W., 2019. A new empirical formula for evaluating uniaxial compressive strength using the Schmidt hammer test. Int. J. Rock Mech. Min. Sci. 123, 104094.
Wang, M., Wan, W., Zhao, Y., 2020. Prediction of the uniaxial compressive strength of rocks from simple index tests using a random forest predictive model. Compt. Rendus Mec. 348 (1), 3–32.
Wang, M., Zhao, G., Liang, W., Wang, N., 2023. A comparative study on the development of hybrid SSA-RF and PSO-RF models for predicting the uniaxial compressive strength of rocks. Case Stud. Constr. Mater. 18, e02191.
Wei, M., Meng, W., Dai, F., Wu, W., 2022. Application of machine learning in predicting the rate-dependent compressive strength of rocks. J. Rock Mech. Geotech. Eng. 14 (5), 1356–1365.
Xiao, P., Li, D., Zhao, G., Liu, H., 2021. New criterion for the spalling failure of deep rock engineering based on energy release. Int. J. Rock Mech. Min. Sci. 148, 104943.
Zhao, R., Shi, S., Li, S., Guo, W., Zhang, T., Li, X., Lu, J., 2023. Deep learning for intelligent prediction of rock strength by adopting measurement while drilling data. Int. J. GeoMech. 23 (4), 04023028.
Zhao, T., Song, C., Lu, S., Xu, L., 2022. Prediction of uniaxial compressive strength using fully bayesian Gaussian process regression (fB-GPR) with model class selection. Rock Mech. Rock Eng. 55 (10), 6301–6319.
Zhou, Z.-H., 2019. Ensemble Methods: Foundations and Algorithms. Chapman and Hall/CRC.